Available online at www.sciencedirect.com
ScienceDirect
Journal of Molecular Structure 875 (2008) 219–225
Journal of MOLECULAR STRUCTURE
www.elsevier.com/locate/molstruc

Ruthenium(II) complexes containing *N*(4)-tolyl-2-acetylpyridine thiosemicarbazones and phosphine ligands: NMR and electrochemical studies of *cis–trans* isomerization

Angelica E. Graminha [a], Alzir A. Batista [a], Javier Ellena [b], Eduardo E. Castellano [b], Letícia R. Teixeira [c,*], Isolda C. Mendes [d], Heloisa Beraldo [d]

[a] *Departamento de Química, Universidade Federal de São Carlos, 1365-905 São Carlos, Brazil*
[b] *Instituto de Física de São Carlos, Universidade de São Paulo, 13560-970 São Carlos, Brazil*
[c] *Departamento de Química, Pontifícia Universidade Católica do Rio de Janeiro, 22653-900 Rio de Janeiro, Brazil*
[d] *Departamento de Química, Universidade Federal de Minas Gerais, 31270-901 Belo Horizonte, Brazil*

Received 22 January 2007; received in revised form 11 April 2007; accepted 20 April 2007
Available online 27 April 2007

Abstract

[Ru(HL)(PPh_3)$_2$Cl]Cl complexes have been obtained in which HL = *N*(4)-*ortho* (complex **1**), *N*(4)-*meta* (complex **2**) and *N*(4)-*para*-tolyl 2-acetylpyridine thiosemicarbazone (complex **3**). NMR and electrochemical studies indicate that both *cis* and *trans* isomers exist in solution, and that the *cis* isomers are converted into the *trans* isomers with time. Crystal structure determination of (**1**) reveals that the *trans* isomer is formed in the solid state.

Keywords: *N*(4)-Tolyl thiosemicarbazones; Ruthenium; Phosphines; *Cis–trans* isomerization

1. Introduction

Thiosemicarbazones and their metal complexes are known for their wide pharmacological versatility [1]. The antitumoral activity of α(*N*)-heterocyclic thiosemicarbazones derived from 2-formyl and 2-acetylpyridine has been extensively investigated as well as the role of coordination on their mechanisms of action [2,3]. Structure–activity relationship studies revealed that the presence of a bulky group attached to the terminal nitrogen of the thiosemicarbazone chain strongly enhances the pharmacological activity of these compounds [4].

Ruthenium complexes are also known for their antitumoral properties and the possibility of producing ruthenium-based compounds for the treatment of cancer is presently under investigation by many groups [5–8]. Therefore the preparation of ruthenium complexes with thiosemicarbazones could be an interesting strategy of combining the pharmacological properties of the ligand with that of the metal in one same compound.

The discovery that the anti-arthritic drug triethylphosphine(2,3,4,6-tetra-*O*-acetyl-β-1-D-thiopyranosato-*S*)gold(I) (auranofin) had antitumoral activity led to the study of other metal complexes containing phosphine ligands. A variety of triphenylphosphine complexes have shown to exhibit significant pharmacological activity [9,10].

In the present work, ruthenium(II) complexes containing *N*(4)-*ortho*-, *N*(4)-*meta* and *N*(4)-*para*-tolyl 2-acetylpyridinethiosemicarbazone (Fig. 1) and triphenylphosphine as ligands have been obtained. NMR and electrochemical studies of *cis–trans* isomerization were carried out. The pharmacological profile of these complexes is presently under investigation.

* Corresponding author. Tel.: +55 21 3527 1813; fax: +55 21 3527 1637.
E-mail address: lregina@qui.puc-rio.br (L.R. Teixeira).

0022-2860/$ - see front matter © 2007 Elsevier B.V. All rights reserved.
doi:10.1016/j.molstruc.2007.04.032

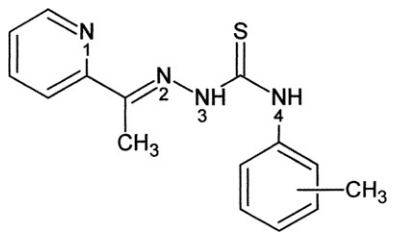

Fig. 1. General structure of *N*(4)-*ortho* (H2Ac4oT), *N*(4)-*meta* (H2Ac4mT) and *N*(4)-*para*-tolyl-2-acetylpyridine thiosemicarbazone (H2Ac4pT).

2. Experimental

2.1. Synthesis

The thiosemicarbazones were prepared as described in the literature [11]. Briefly, 2-acetylpyridine (6 mmol) was added to a slight excess of hydrazine hydrate in ethanol under reflux. The resulting hydrazone (5 mmol) was added to *ortho-meta-* or para-tolyl isothiocianate (5 mmol) in ethanol under reflux. The solids which precipitated were filtered and washed with isopropanol then diethylether and dried.

The complexes were obtained by dissolving the desired thiosemicarbazone (0.20 mmol) in CH_2Cl_2(20 mL) with gentle heating under argon atmosphere. After cooling the solution to room temperature [$RuCl_2(PPh_3)_3$] (0.20 mmol) was added. The complexes which form immediately precipitate by addition of diethyl ether. The solids were filtered and washed with methanol and diethyl ether and dried *in vacuo*.

[Ru(H2Ac4oT)$(PPh_3)_2$Cl]Cl (**1**): Yield: 0.140 g (71.4%). Anal. Calc: C, 62.45; H, 4.73; N, 5.71%. Found: C, 62.22; H, 4.69; N, 5.68 %. Molar conductivity ($\mu S\ cm^{-1}$): 33.85 (CH_2Cl_2). IR (KBr ν/cm^{-1}): 1556 (C=N); 746 (C=S); 620 (ρpy); 531, 521 (Ru–P); 498 (Ru–N); 417 (Ru–S); 284 (Ru–N_{PY}); 332 (Ru–Cl). ^1H NMR ($CDCl_3$ δ/ppm): 13.25, 12.70 (s, 1H, N(2)–H); 10.94, 10.62 (s, 1H, N(4)–H); 2.57, 2.31 (s, 3H, C(7)H_3); 2.07, 2.05 (s, 3H, C(15)H_3). $^{31}P\{^1H\}$ NMR (CH_2Cl_2 δ/ppm): 24.4 (s); 41.2 (d, $^2J_{P-P}$/Hz 28.9); 38.5 (d, $^2J_{P-P}$/Hz 28.8).

[Ru(H2Ac4mT)$(PPh_3)_2$Cl]Cl (**2**): Yield: 0.148 g (75.5%). Anal. Calc: C, 62.45; H, 4.73; N, 5.71%. Found: C, 61.96; H, 4.71; N, 5.67 %. Molar conductivity ($\mu S\ cm^{-1}$): 34.15 (CH_2Cl_2). IR (KBr ν/cm^{-1}): 1556 (C=N); 744 (C=S); 618 (ρpy); 525, 520 (Ru–P); 499 (Ru–N); 418 (Ru–S); 305 (Ru–N_{PY}); 329 (Ru–Cl).^1H NMR ($CDCl_3$ δ/ppm): 12.88, 12.11 (s, N(2)–H); 11.45, 11.09 (s, N(4)–H); 2.51, 2.28 (s, 3 H, C(7)H_3); 2.19, 2.03 (s, 3H, C(15)H_3). $^{31}P\{^1H\}$ NMR (CH_2Cl_2 δ/ppm): 23.8 (s); 41.2 (d, $^2J_{P-P}$/Hz 28.3); 39.0 (d, $^2J_{P-P}$/Hz 28.6).

[Ru(H2Ac4pT)$(PPh_3)_2$Cl]Cl (**3**): Yield: 0.136 g (69.4%). Anal. Calc: C, 62.45; H, 4.73; N, 5.71%. Found: C, 62.01; H, 4.70; N, 5.67 %. Molar conductivity ($\mu S\ cm^{-1}$): 33.65. IR (KBr ν/cm^{-1}): 1553 (C=N); 745 (C=S); 619 (ρpy); 533, 520 (Ru–P); 498 (Ru–N); 418 (Ru–S); 288 (Ru–N_{PY}); 324 (Ru–Cl). ^1H NMR ($CDCl_3$ δ/ppm): 12.89, 12.09 (s, N(2)–H); 11.42, 11.04 (s, N(4)–H); 2.51, 2.27 (s, 3H, C(7)H_3); 2.22, 2.06 (s, 3H, C(15)H_3). $^{31}P\{^1H\}$ NMR (CH_2Cl_2 δ/ppm): 23.3 (s); 40.8 (d, $^2J_{P-P}$/Hz 28.7); 38.6 (d, $^2J_{P-P}$/Hz 29.0).

2.2. Physical measurements

Elemental analyses were performed on a Fison equipment, model EA 1108. A Radiometer Copenhagem Meter Lab., model CDM 230 was employed for molar conductivity measurements. Infrared spectra (KBr pellets) were obtained using a BOMEM MICHELSON instrument, model 102. NMR spectra were obtained at room temperature with a Brucker DRX-400 Avance (400 MHz) spectrometer. For ^1H measurements $CDCl_3$ was used as solvent and tetramethylsilane (TMS) as internal reference and for $^{31}P\{^1H\}$ (161 MHz) CH_2Cl_2 was used as solvent and H_3PO_4 85% as external reference.

The electrochemical experiments were carried out at room temperature in dichloromethane containing 0.1 mol L^{-1} tetrabutylammoniumperchlorate (TBAP, Fluka Purum) using an electrochemical analyzer from Bioanalytical Systems Inc. (BAS), model 100BW. The working and auxiliary electrodes were stationary Pt foils, and the reference electrode was Ag/AgCl, a medium in which ferrocene is oxidized at 0.48 V (Fc^+/Fc).

2.3. X-ray crystallography

Room temperature X-ray diffraction data collection (ϕ scans and ω scans with κ offsets) of *trans*[Ru(H2Ac4oT)$(PPh_3)_2$Cl]Cl was performed on an Enraf-Nonius Kappa-CCD diffractometer (95 mm CCD camera on κ-goniostat) using graphite-monochromated MoKα radiation (0.71073 Å). Data were collected up to 50° in 2θ, with a redundancy of 4. The final unit cell parameters were based on all reflections. Data collections were carried out using the COLLECT program [12]; integration and scaling of the reflections were performed with the HKL Denzo-Scalepack system of programs [13]. Analytical absorption correction was applied [14].

The structure was solved by direct methods with SHELXS-97 [15a]. The model was refined by full-matrix least squares on F^2 with SHELXL-97 [15b]. All hydrogen atoms were stereochemically positioned and refined with the riding model [15b]. Hydrogen atoms of the CH groups were set isotropic with a thermal parameter 20% greater than the equivalent isotropic displacement parameter of the atom to which each one was bonded. This percentage was set to 50% for the hydrogen atoms of the CH_3 group. The programs SHELXL-97 [15b], and ORTEP-3 [16] were used within WinGX [17] to prepare materials for publication.

3. Results and discussion

Microanalyses and molar conductivity data suggest the formation of [Ru(H2Ac4oT)$(PPh_3)_2$Cl]Cl (**1**),

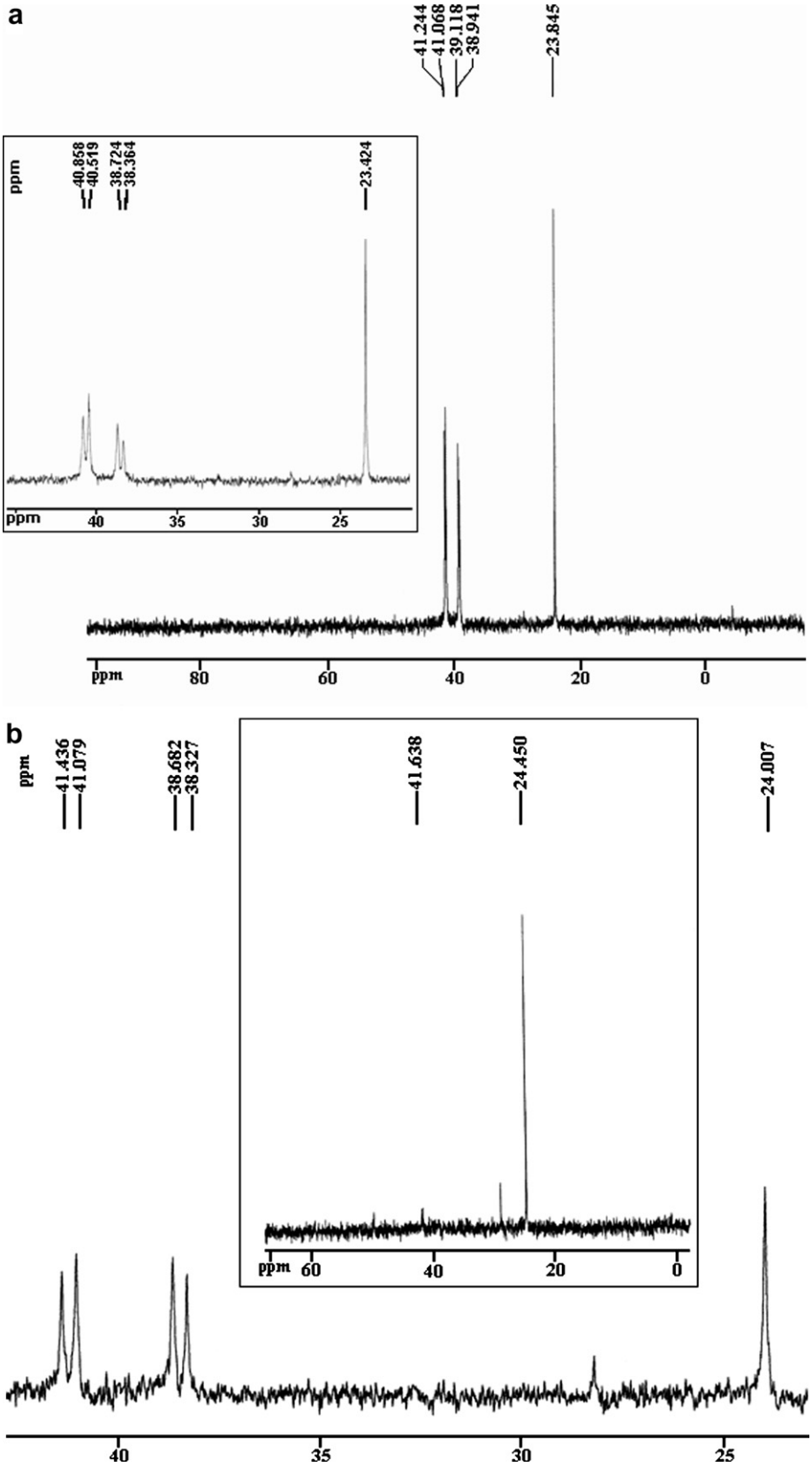

Fig. 2. $^{31}P\{^{1}H\}$ NMR spectra of (a) *cis*/*trans*[RuCl(H2Ac4mT)(PPh_3)$_2$]Cl and (b) *cis*/*trans*[RuCl(H2Ac4oT)(PPh_3)$_2$]Cl recorded immediately after dissolution and after 24 h.

Table 1
Cyclic voltammetry data for complexes (**1**)–(**3**) (0.100 V s^{-1}, CH_2Cl_2, 0.1 mol L^{-1} TBAP)

	Process 1 (*cis* isomer)		Process 2 (*trans* isomer)	
	Ru^{II}/Ru^{III} (V)	Ru^{III}/Ru^{II} (V)	Ru^{II}/Ru^{III} (V)	Ru^{III}/Ru^{II} (V)
cis/*trans*[Ru(H2Ac4oT)$(PPh_3)_2$Cl]Cl (**1**)	0.47	0.37	0.78	0.60
cis/*trans*[Ru(H2Ac4mT)$(PPh_3)_2$Cl]Cl (**2**)	0.47	0.31	0.75	0.57
cis/*trans*[Ru(H2Ac4pT)$(PPh_3)_2$Cl]Cl (**3**)	0.48	0.29	0.75	0.58

[Ru(H2Ac4mT)$(PPh_3)_2$Cl]Cl (**2**) and [Ru(H2Ac4pT)$(PPh_3)_2$Cl]Cl (**3**). The molar conductivity data indicate that all complexes are 1:1 electrolytes, in accordance with the proposed formulations.

3.1. IR spectral studies

In the infrared spectra, the *v*(C=N) stretching vibration of the thiosemicarbazones at 1580–1582 cm^{-1} shifts to 1553–1556 cm^{-1} in the complexes, indicating coordination of the imine nitrogen [18,19]. The absorption at 782–796 cm^{-1} in the spectra of the free ligands, attributed to the *v*(C=S) vibration, shifts to 744–746 cm^{-1}(37–50 cm^{-1}) in the spectra of the complexes, indicating complexation through a thione sulfur [20]. The in-plane deformation mode of the pyridine ring observed in the 590–608 cm^{-1}region in the spectra of the uncomplexed thiosemicarbazones shifts to 618–620 cm^{-1} in the spectra of the complexes, in accordance with coordination through the heteroaromatic nitrogen [18–20]. Two absorptions at 520–533 cm^{-1}were attributed to the *v*(Ru–P) mode which is split, indicating the presence of two phosphorus atoms in *cis* position to each other. However, since a *trans* isomer would present a single absorption attributed to *v*(Ru–P) in the same region, the presence of both *cis* and *trans* isomers in the powder cannot be discarded. Absorptions at 498–499 cm^{-1}, 417–418 cm^{-1} and 284–305 cm^{-1} in the spectra of the complexes were attributed to the *v*(Ru–N), *v*(Ru–S) and *v*(Ru–N_{py}), vibrations [21], indicating coordination of the thiosemicarbazones through the N_{py}–N–S chelating system. Absorptions at 324–332 cm^{-1} in the spectra of the complexes were attributed to the *v*(Ru–Cl) vibration [21].

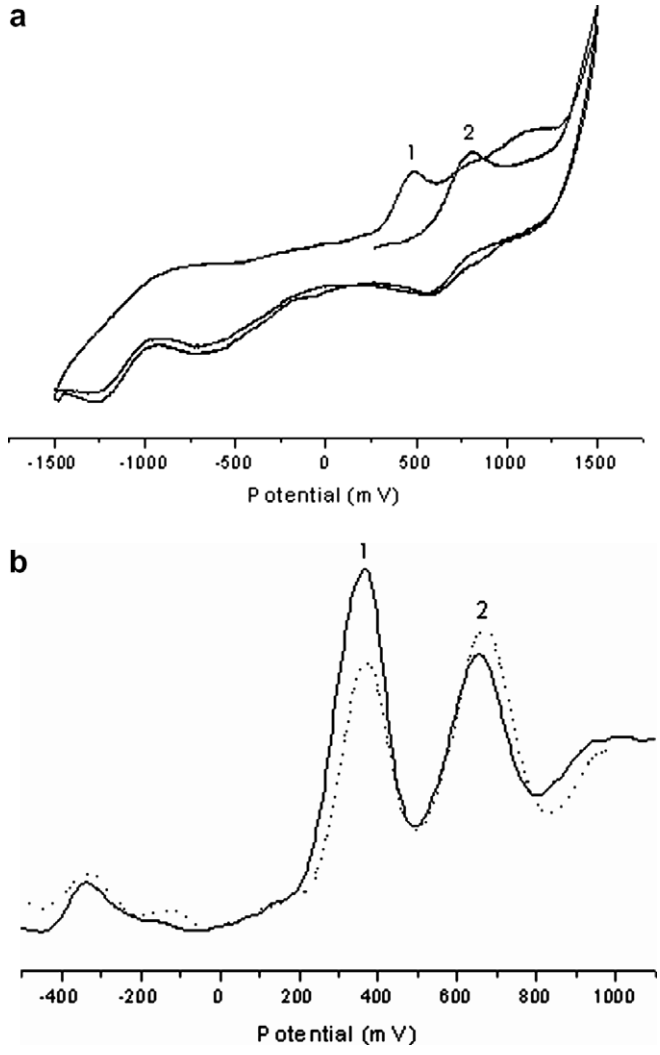

Fig. 3. (a) Cyclic voltammogramm and (b) Differential pulse voltammogram of *cis*/*trans*[RuCl(H2Ac4oT)$(PPh_3)_2$]Cl (wave 1 corresponds to the *cis* isomer and wave 2 to the *trans* isomer, CH_2Cl_2, 0.1 mol L^{-1} TBAP); (—) immediately after dissolution and (- -) 10 min after dissolution.

3.2. NMR spectral studies

$^{31}P\{^1H\}$ NMR spectra of complexes (**1**)–(**3**) (using CH_2Cl_2 as solvent) have been recorded immediately after dissolution and after 24 h. In the $^{31}P\{^1H\}$ NMR spectra of (**1**)–(**3**) the singlet at δ23.3–δ24.4 was attributed to *trans*[Ru(HL)$(PPh_3)_2$Cl]Cl (HL = *N*(4)-*o*-, *N*(4)-*m* or *N*(4)-*p*-tolyl 2-acetylpyridine thiosemicarbazone) and the two doublets at δ38.5–41.2 ($^2J_{P-P} = 29$ Hz) were assigned to the corresponding *cis* complexes, in which one phosphorus atom is *trans* to the chloride ligand and the second is *trans* to the imine nitrogen of the thiosemicarbazone chain. In all cases the intensities of the two doublets decrease with time, suggesting conversion of the *cis* to the *trans* isomer, probably due to sterical effects that favor the formation of the *trans* isomeric form. For complexes (**2**) and (**3**) the $^{31}P\{^1H\}$ NMR spectra immediately after dissolution indicated predominance of the *trans* isomer (67%). After 24 h 75% of the *trans* isomer exist in solution (see Fig. 2a). Similarly, in the case of complex (**1**) the *trans* isomer predominates (61%) immediately after dissolution. After 24 h only the *trans* isomer is present, suggesting that in this case *cis*–*trans* conversion is faster (see Fig. 2b).

Table 2
Crystal data, structure solution methods and refinement results for *trans*[Ru(H2Ac4oT)(PPh_3)$_2$Cl]Cl (**1**)

Empirical formula	$C_{51}H_{46}N_4P_2SCl_2Ru$	
Formula weight	980.93	
Temperature	293(2) K	
Wavelength	0.71073 Å	
Crystal system	Monoclinic	
Space group	$P2_1/n$	
Unit cell dimensions	$a = 9.7090(10)$ Å	
	$b = 40.210(4)$ Å	$\beta = 90.163(7)°$
	$c = 11.917(2)$ Å	
Volume	4652.4(10) Å^3	
Z	4	
Density (calculated)	1.399 Mg/m^3	
Absorption coefficient	0.605 mm^{-1}	
$F(000)$	2012	
Crystal size	$0.43 \times 0.08 \times 0.02$ mm^3	
Theta range for data collection	3.10–25.00°	
Index ranges	$-11 \leqslant h \leqslant 11$, $-11 \leqslant k \leqslant 47$, $-14 \leqslant /\leqslant 14$	
Reflections collected	14196	
Independent reflections	7340 [R(int) = 0.1553]	
Completeness to theta = 25.00°	89.8%	
Absorption correction[1]	Gaussian	
Max. and min. transmission	0.988 and 0.912	
Refinement method	Full-matrix least squares on F^2	
Data/restraints/parameters	7340/0/552	
Goodness-of-fit on F^2	1.065	
Final R indices [$I > 2\sigma(I)$]	$R1 = 0.0965$, w$R2 = 0.2516$	
R indices (all data)	$R1 = 0.1712$, w$R2 = 0.2833$	
Largest diff. peak and hole	1.066 and −0.753 e Å^{-3}	

[a]Data collection, data processing, structure solution and structure refinement, respectively.

The ^{1}H NMR spectra of the thiosemicarbazones in $CDCl_3$ show a singlet at δ9.30 which is attributed to N(2)–H. This signal appears duplicated at δ12.09–13.25 range in the spectra of (**1**)–(**3**) in accordance with the presence of the *cis* and *trans* isomers in solution. The signal at δ8.80 in the spectra of the thiosemicarbazones was attributed to N(4)–H. Similarly two signals of N(4)–H at δ10.62–11.45 were observed in the spectra of (**1**)–(**3**), which have been assigned to the *cis* and *trans* isomers. In addition, four signals were present in the spectra of the complexes, attributed to the methyl hydrogens of the acetyl and tolyl groups of the *cis* and *trans* isomers. In the spectrum of (**1**) the signals at δ2.29 and 2.05 were assigned to the acetyl and tolyl hydrogens of the *trans* isomer and those at δ 2.57 and 2.07 to these hydrogens of the *cis* isomer. In the spectrum of (**2**) the acetyl and tolyl hydrogens were found at δ2.28 and δ2.19, respectively (*trans* isomer), and at δ2.51 and δ2.03 (*cis* isomer) and in the spectrum of (**3**) the acetyl and tolyl hydrogens were found at δ2.27 and δ2.22, respectively (*trans* isomer), and at δ2.51 and δ2.06, respectively (*cis* isomer).

Crystal structure determination of (**1**) (see below) reveals that the *trans* isomer is obtained, confirming that the *trans* species is indeed the thermodynamically most stable. As mentioned before, infrared data have indicated that either the *cis* isomer or both *cis* and *trans* isomers were present in the powder. Since the $^{31}P\{^1H\}$ NMR spectra immediately after dissolution already showed the presence of both isomers, we may infer that the two compounds were present in the powder. Only the *trans* isomer crystallized from the filtrate.

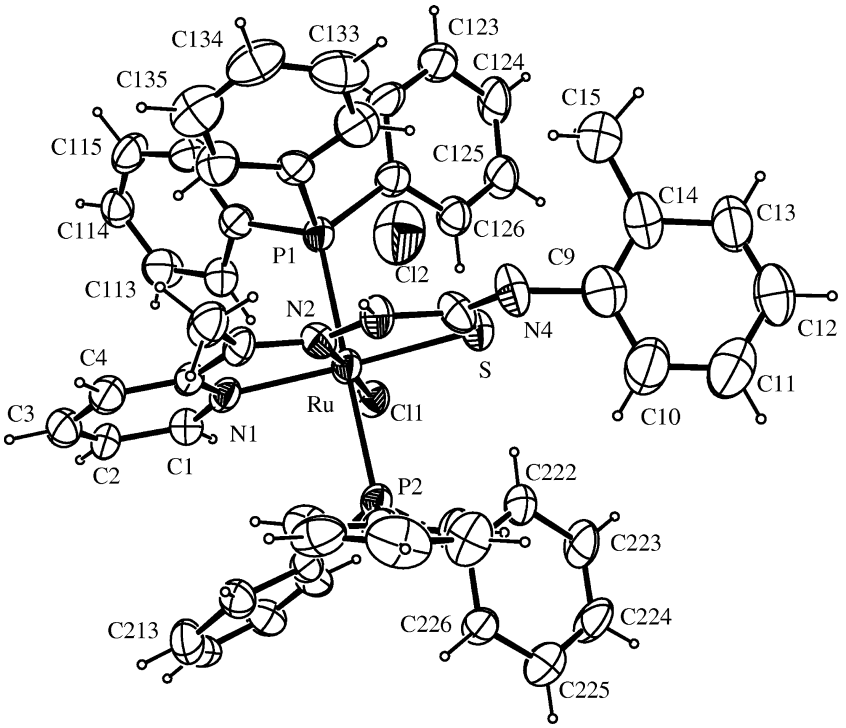

Fig. 4. ORTEP view of *trans*[Ru(H2Ac4oT)(PPh_3)$_2$Cl]Cl, showing the labeling of the non-hydrogen atoms and their displacement ellipsoids at the 50% level.

Interestingly other authors have reported a study of complex (**3**) [22] but did not report $^{31}P\{^{1}H\}$ NMR spectra and did not mention the *cis–trans* isomerization process reported by the first time in the present investigation.

3.3. Electrochemical studies

Table 1 shows the electrochemical data for (**1**)–(**3**). The voltammograms exhibit two quasi-reversible processes attributed to the Ru^{II}/Ru^{III} oxidation (Fig. 3a). The first process in the 0.29–0.48 V range, which disappears with time is assigned to the *cis* isomer. The second, which occurs in the 0.57–0.78 V range, becomes more intense, as observed in the differential pulse voltammograms, and was attributed to the *trans* isomer (see Fig. 3b). Two consecutive reduction waves were observed in the −0.67 to −0.70 V and in the −1.27 to −1.42 V ranges, which have been assigned to redox processes of the thiosemicarbazone. These two reduction signals could be assigned to a two-step two-electron reduction process involving first the cleavage of the N–N single bond by reduction with two electrons and then reduction by two electrons at the imine formed, as suggested for pyridine-derived thiosemicarbazones and semicarbazones [23–25].

The previously published study of complex (**3**) [22] reported the electrochemical behavior of the complex but did not mention the presence of *cis–trans* isomers in solution, which were clearly evidenced in the present investigation.

At this point it is worth noticing that while in the present study the preparations of complexes (**1**)–(**3**) were carried out at room temperature, in the previously published work the synthesis of complex (**3**) was carried out under reflux (4 h). These conditions could have favored complete conversion of the *cis* to the *trans* isomer.

3.4. Crystal structure of trans[Ru(H2Ac4oT)(PPh$_3$)$_2$Cl]Cl

Crystal data and refinement results for *trans*[Ru(H2Ac4oT)(PPh$_3$)$_2$Cl]Cl (**1**) are shown in Table 2. Fig. 4 is the ORTEP3 view of the molecule. Table 3 shows selected bond distances [Å] and angles [°]. The structure was refined in the monoclinic system, $P2_1/n$ with four molecules in the asymmetric unit.

Table 3
Selected bond lengths [Å] and angles [°] for *trans*[Ru(H2Ac4oT)(PPh$_3$)$_2$Cl]Cl

S–C(8)	1.726(14)	N(2)–N(3)–C(8)	118.3(11)
N(2)–C(6)	1.346(15)	N(3)–C(8)–S(1)	120.5(10)
N(2)–N(3)	1.366(13)	N(4)–C(8)–N(3)	113.1(12)
N(3)–C(8)	1.366(16)	N(4)–C(8)–S(1)	126.4(11)
N(4)–C(8)	1.330(16)	C(6)–N(2)–N(3)	119.2(10)
N(4)–C(9)	1.50(2)	C(8)–N(4)–C(9)	120.5(12)
Ru–N(2)	1.985(11)	N(2)–Ru–N(1)	78.8(4)
Ru–N(1)	2.118(10)	N(1)–Ru–S	161.4(3)
Ru–P(1)	2.410(4)	P(2)–Ru–P(1)	176.19(13)
Ru–P(2)	2.381(4)	N(2)–Ru–Cl(1)	177.0(3)
Ru–S	2.386(3)	N(1)–Ru–Cl(1)	98.4(3)
Ru–Cl(1)	2.449(3)		

The structure of complex (**1**) reveals that the thiosemicarbazone coordinates through the N_{py}–N(2)–S chelating system. The remaining coordination positions are occupied by two triphenylphosphine groups *trans* to each other and a chloride which is *trans* to N(2).

Distortion from perfect octahedral geometry is caused by N(1), which is 0.11(1) Å apart from the plane formed by Ru, N2 and Cl1. The angle formed by the line through P1 and P2 with this plane is 2.2(1)° and the P1–Ru–P2 bond angle is 176.2(1)°.

Analyses of the supra-molecular organization shows an intermolecular interaction between N3–H3...Cl2 (N3..Cl2 = 3.056(1) Å, H3...Cl2 = 2.289(4)Å, N3–H3....Cl2 = 148.6(7)°) that fixes the position of the chloride ion.

Other authors determined the crystal structure of *trans*[-Ru(H2Ac4pT)(PPh$_3$)$_2$Cl]Cl (complex (**3**) of the present paper) [22]. Comparison between the structures of the two complexes reveals some differences in bond distances and angles. The C8–S bond distance is 1.726(14) Å in (**1**) and 1.706(6) Å in (**3**); the C8–N3 bond distance is 1.366(16) Å in (**1**) and 1.359(7) Å in (**3**); the N2–N3 bond distance is 1.366(13) Å in (**1**) and 1.383(7) Å in (**3**). The Ru–N(1) bond distance is 2.118(10) Å in (**1**) and 2.085(5) Å in (**3**). In (**1**) the Ru–P1 distance is 2.410(4) Å and the Ru–P2 distance is 2.381(4) Å whereas the two Ru–P distances are equal (2.399(1) Å) in (**3**).

The N2–Ru–N1 angle is 78.8(4)° in complex (**1**) and 77.4(2)° in (**3**); the N1–Ru–S angle is 161.4(3)° in (**1**) and 160.8(1)° in (**3**) and P2–Ru–P1 is 176.19(13)° in (**1**) and 175.2(1)° in (**3**).

Acknowledgement

This work was supported by CNPq and FAPESP of Brazil.

Appendix A. Supplementary data

Listings of fractional coordinates and equivalent isotropic displacement parameters (Tables 1S), full bond distances and angles (Tables 2S), atomic anisotropic displacement parameters (Table 3S), hydrogen atoms positions (Table 4S) and complete list of torsion angles (Tables 5S). Crystallographic data for complex (1) have been deposited at Cambridge Crystallographic Data Centre as supplementary publication number CCDC 632565. Copies of available material can be obtained on application to CCDC, 12 Union Road, Cambridge CB2 1Ez, UK (fax: 44 1223 336033 or e-mail: deposit@ccdc.cam.ac.uk). Supplementary data associated with this article can be found, in the online version, at doi:10.1016/j.molstruc.2007.04.032.

References

[1] H. Beraldo, D. Gambino, Mini. Rev. Med. Chem. 4 (2004) 31.
[2] M.C. Liu, T.S. Lin, A.C. Sartorelli, J. Med. Chem. 35 (1992) 3672.
[3] A.E. Liberta, D.X. West, Biometals 5 (1992) 121.
[4] D.X. West, A. Liberta, S.B. Padhye, R.C. Chikate, P.B. Sonawane, A.S. Kumbhar, R.G. Yerande, Coord. Chem. Rev. 123 (1993) 49.
[5] C.X. Zhang, S.J. Lippard, Curr. Opin. Chem. Biol. 7 (2003) 481.
[6] R.A. Vilaplana, F. Delmani, C. Manteca, J. Torreblanca, J. Moreno, G. García-Herdugo, F. González-Vílchez, J. Inorg. Biochem. 100 (2006) 1834.
[7] V. Brabec, O. Nováková, Drug Resist. Updat. 9 (2006) 111.
[8] D. Chatterjee, A. Sengupta, A. Mitra, S. Basak, Inorg. Chim. Acta 358 (2005) 2954.
[9] N. Farrel, Transition Metal Complex as Drug and Chemotherapeutic Agents, Kluwer, Dordrecht, 1989.
[10] R.C. Elder, R. Ludwig, J.N. Cooper, M.K. Eidness, J. Am. Chem. Soc. 107 (1985) 5024.
[11] I.C. Mendes, J.P. Moreira, N.L. Speziali, A.S. Mangrich, J.A. Takahashi, H. Beraldo, J. Braz. Chem. Soc. 17 (2006) 1571.
[12] Enraf-Nonius (1997–2000). COLLECT. Nonius BV, Delft, The Netherlands.
[13] Z. Otwinowski, W. Minor, in: C.W. CarterJr., R.M. Sweet (Eds.), Methods in Enzymology, 276, Academic Press, New York, 1997, pp. 307–326.
[14] P. Coppens, L. Leiserowitz, D. Rabinovich, Acta Cryst. 18 (1965) 1035G.
[15] (a) M. Sheldrick, SHELXS-97. Program for Crystal Structure Resolution, University of Göttingen, Göttingen, Germany, 1997;
(b) M. Sheldrick, SHELXL-97. Program for Crystal Structures Analysis, University of Göttingen, Göttingen, Germany, 1997.
[16] L.J. Farrugia, J. Appl. Cryst. 30 (1997) 565.
[17] L.J. Farrugia, J. Appl. Cryst. 32 (1999) 837.
[18] H. Beraldo, W.F. Nacif, L.R. Teixeira, J.S. Rebouças, Transit. Met. Chem. 27 (2002) 85.
[19] A.P. Rebolledo, G.M. de Lima, L.N. Gambi, N.L. Speziali, D.F. Maia, C.B. Pinheiro, J.D. Ardisson, M.E. Cortés, H. Beraldo, Appl. Organometal. Chem. 17 (2003) 945.
[20] P. Sengupta, R. Dinda, S. Ghosh, W. Sheldrick, Polyhedron 22 (2003) 447.
[21] K. Nakamoto, Infrared and Raman Spectra of Inorganic and Coordination Compounds, fourth ed., Wiley, New York, 1986.
[22] M. Maji, M. Chatterjee, S. Ghosh, S.K. Chattopadhyay, Bo-Mu Wu, T.C.W. Makc, J. Chem. Soc., Dalton Trans. (1999) 135.
[23] M.M.B. Pessoa, G.F.S. Andrade, M.R. dos Santos, M.L.A. Temperini, J. Electroanal. Chem. 545 (2003) 117 (and references therein).
[24] A. Perez-Rebolledo, O.E. Piro, E.E. Castellano, Letícia R. Teixeira, A.A. Batista, H. Beraldo, J. Molec. Struct. 794 (2006) 18.
[25] R.P. John, A. Sreekanth, V. Rajakannan, T.A. Ajith, M.R. Prathapachandra Kurup, Polyhedron 23 (2004) 2549.